

Azimuthal asymmetries for quark pair production in pA collisions

Emin Akcakaya, Andreas Schäfer and Jian Zhou

Institut für Theoretische Physik, Universität Regensburg, Regensburg, Germany

September 3, 2019

Abstract

We study the azimuthal asymmetries for quark pair production in proton-nucleus collisions using a hybrid approach in which the nucleus is treated in the Color Glass Condensate (CGC) framework while the Lipatov approximation is applied on the proton side. Our treatment goes beyond the large N_c limit. We particularly focus on the so-called correlation limit where the imbalance of the transverse momentum of the quark pair is much smaller than the out-going individual quark transverse momenta. In this kinematic region, a matching between the hybrid approach and a factorization in terms of transverse momentum dependent parton distributions (TMDs) has been found. It is shown which of the various unpolarized and linearly polarized gluon TMD distributions contribute to $\cos 2\phi$ and $\cos 4\phi$ modulations of quark pair production.

1 Introduction

During the past three decades, transverse momentum dependent (TMD) factorization framework has been systematically developed (TMDs) [1, 2]. While many theoretical tools have been developed and were applied to a wide selection of hard scattering processes (see, for example Refs. [3, 4] and references therein) and much insight was gained, a formalism which would be on the one side complete and in all aspects well-defined and on the other side easily applicable to all processes has not yet been found. Therefore, one still has often to resort to models (like the one used here) for the practical calculations. In fact, it seems as if di-jet production in hadron-hadron collisions [5, 6] is one of the especially problematic cases. Recently, however, an effective TMD factorization has been established at small x for di-jet production in nucleon-nucleus collisions [7, 8]. This was achieved by extrapolating the full Color Glass Condensate (CGC) result to the so-called correlation limit where the k_\perp -imbalance of di-jets is much smaller than each of the jet transverse momenta. The key observation was that in the correlation limit, two out-going jets stay very close in position space, such that multiple-point functions appearing in the CGC formalism collapse into the two point function. The derivative of the two point function with respect to the transverse coordinate was related to the various gluon TMDs. Following this line of argument one would conclude that the basic building blocks are gluon multiple-point functions, namely Wilson line, rather than gluon TMDs. Note that the multiple soft gluon interaction between the nucleon and the active partons is neglected in the CGC calculation since the background gluon field inside a large nucleus is much stronger than that inside a nucleon. This leads to the absence of contributions causing a violation of generalized TMD factorization [6]. A comprehensive review covering among others the relation between the CGC formalism and TMD factorization can be found in Ref. [9].

In this paper, following the same spirit, we study quark pair production in the correlation limit in pA collisions, with special focus on the polarized case. Quark pair production in high energy hadron-hadron collisions has been investigated in the framework of collinear factorization in [10, 11] and in

k_\perp factorization in [12–14]. Later, a CGC calculation has shown that for quark pair production in nucleon-nucleus collisions, the result for k_\perp factorization can be recovered from the CGC one in the dilute limit where the gluon densities are not too high, but that this fails in a dense medium [15, 16]. In addition to the two point function, three point functions and four point functions also show up in the CGC calculation. These multiple-point functions provide a deep access into the saturation physics in the kinematical region beyond the correlation limit.

We will first reproduce the full CGC result using a hybrid approach [17] in which the nucleus is treated in the Color Glass Condensate (CGC) framework [18, 19] while the Lipatov approximation [12, 13, 20, 21] is applied on the proton side. The second step is to extrapolate this result to the correlation limit by using a power expansion of the hard coefficients. The fact that the hard coefficients become independent of the gluon transverse momentum enables us to integrate out one or two gluon transverse momenta. Correspondingly, the three point functions and four point functions collapse and can be expressed as derivatives of the two point function. The latter can be related to the various gluon TMDs. Using the different polarization tensor structures, the gluon TMDs are classified into an unpolarized gluon distribution and the distribution of linearly polarized gluons. The latter one is responsible for $\cos 2\phi$ and $\cos 4\phi$ azimuthal asymmetries for quark pair production in proton-nucleus collisions.

The linearly polarized gluon distribution [22, 23] ($h_1^{\perp g}$ in the notation of Ref. [24]) recently has attracted quite a lot of attention. It is the only spin dependent gluon TMD for an unpolarized nucleon/nucleus, and may be considered as the counterpart of the quark Boer-Mulders function $h_1^{\perp q}(x, k_\perp)$ [25]. However, in contrast to the latter, $h_1^{\perp g}$ is time-reversal even implying that initial/final state interactions are not needed for its existence [26, 27]. Despite this fact, it does receive the contributions from the initial/final state interaction, leading to the process dependent gauge links. This distribution function is of phenomenological interest, especially for small- x physics at RHIC and LHC because a calculation in the saturation model [28] showed that its contributions are (at small- x) as large as those proportional to the unpolarized gluon distribution. The saturation model calculation also reveals that the linearly polarized gluon distributions with different gauge link structures differ significantly at low transverse momentum, though they all recover the normal perturbative tail at high transverse momentum.

A few ways of accessing $h_1^{\perp g}$ have been put forwarded, namely through measuring azimuthal $\cos 2\phi$ asymmetries in processes such as jet or quark pair production in electron-nucleon scattering as well as nucleon-nucleon scattering [29, 30]. Other promising observables are $\cos 2\phi$ asymmetries in photon pair production in hadron collisions [31] and in virtual photon-jet production in nucleon nucleus collisions [28]. Such measurements should be feasible at RHIC, LHC, and a potential future Electron Ion Collider (EIC) [3, 4]. More recently, it has been found that the linearly polarized gluon distribution may affect the transverse momentum distribution of Higgs bosons produced from gluon fusion [17, 32, 33], color-neutral particles produced in nucleus-nucleus collisions [34], and heavy quarkonium produced in hadronic collisions [35]. The authors of Ref. [32] proposed that the effect of linearly polarized gluons on the Higgs transverse momentum distribution can even be used, in principle, to determine the parity of the Higgs boson experimentally. Transverse momentum dependent factorization has been re-examined by taking into account the perturbative gluon-radiation correction to $h_1^{\perp g}$ [33]. The complete TMD factorization results for Higgs boson production are consistent with earlier findings based on the Collins-Soper-Sterman (CSS) formalism [36] and soft-collinear-effective theory [37]. Also, the transverse momentum resummation formalism applied to di-photon production in pp collisions [38] is closely related. The recent development [39] has shown that it might be also promising to perform the resummation procedure on the light-cone.

The article is organized as follows. In the next section, we start by reviewing our version of the hybrid approach which allows us to describe effects caused by the finite gluon transverse momentum

on the proton side. Then we reproduce the known result for the quark pair production amplitude in pA collisions using this hybrid approach. The next step is a power expansion in the correlation limit. We show that the resulting differential cross section depends only on gluon TMDs rather than higher multiple-point functions. We particularly focus on the polarized cross section which contains the linearly polarized gluon distributions. Our treatment goes beyond the large N_c limit used in earlier studies. In section III, we discuss our result in the dilute limit, the forward limit and the large N_c limit. It is shown that our expressions are consistent with the existing results in these different limits. In section IV, we re-derive the cross section in the TMD factorization framework. As expected, a matching between the CGC formalism and the TMD factorization approach is found in the correlation limit. In the end, we summarize our results.

2 Quark pair production in the CGC framework

Let us first consider the general case of quark pair production,

$$\mathcal{P}(P_B) + \mathcal{A}(P_A/\text{per nucleon}) \rightarrow q(l_1) + \bar{q}(l_2) + X. \quad (1)$$

We assume that the nucleus is moving with a velocity very close to the speed of light into the positive z direction, while the proton is moving in the opposite direction. It is convenient to use light-cone coordinates for which $P_A^\mu = P_A^+ p^\mu$ and $P_B^\mu = P_B^- n^\mu$ with $p = (1, 0, 0, 0)$ and $n = (0, 1, 0, 0)$. The corresponding partonic subprocess is represented by $g_A(k_1) + g_p(k_2) \rightarrow q(l_1) + \bar{q}(l_2)$, where $k_1^\mu = x_1 P_A^\mu + k_{1T}^\mu$ denotes the total momentum carried by multiple gluons from the nucleus, and $k_2^\mu = x_2 P_B^\mu + k_{2T}^\mu$ is the momentum of the gluon from the proton. In the following the notations $k_{1\perp}$ and $k_{2\perp}$ are used to denote three dimension vectors with $k_{1\perp}^2 = -k_{1T}^2$ and $k_{2\perp}^2 = -k_{2T}^2$. To simplify the calculation, we choose to work in the light-cone gauge of the proton ($A^- = 0$). Correspondingly, the polarization tensor of a gluon carrying the momentum l is given by,

$$\varepsilon^{\mu\nu}(l) = -g^{\mu\nu} + \frac{p^\mu l^\nu + p^\nu l^\mu}{p \cdot l}. \quad (2)$$

As mentioned in the introduction, to facilitate our calculation, a hybrid approach [17] has been adopted, in which the nucleus is treated in the CGC model, while on the side of the dilute projectile proton one makes the so-called Lipatov approximation [12, 13, 20, 21]. At small x , the gluon radiation cascade shows a strong ordering in rapidity. In other words, the radiating color source carries a much larger longitudinal momentum than the radiated gluon. It has been shown that a fast moving color source can be treated as eikonal line in the strongly rapidity ordered region. Making such a replacement is referred to as Lipatov approximation [13].

For the process of gluon production in pA collisions, the relevant eikonal line is the past-pointing one which is built up through initial state interactions between the color sources inside the proton and the background gluon field. The interaction between the classical gluon field and the final state gluon emitted from the color source inside the proton does not change this general statement because the imaginary part of the scattering amplitude cancels between the different cut diagrams once the final states are integrated out. The prescription to treat the eikonal propagator is fixed by this choice. The relevant Feynman rules, illustrated in Fig. 1, were given in Ref. [13]. Note that the prescription for past-pointing eikonal propagators differs from that for future-pointing eikonal lines.

The multiple scattering between the outgoing quark pair and the classical color field of the nucleus can be readily resummed to all orders [40, 41]. This gives rise to a path-ordered gauge factor along the straight line that extends in x^- from minus infinity to plus infinity. More precisely, for a quark with incoming momentum l and outgoing momentum $l + k$, the path-ordered gauge factor reads,

$$2\pi\delta(k^-)p^\mu[U - 1](k_\perp), \quad (3)$$

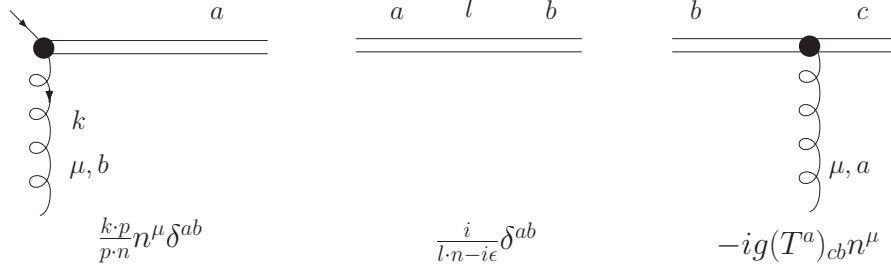


Figure 1: Feynman rules for the eikonal line, which is represented by a double line. a, b and c denote color indices.

with

$$[U - 1](k_\perp) = \int d^2 x_\perp e^{-ik_\perp \cdot x_\perp} [U(x_\perp) - 1], \quad (4)$$

and

$$U(x_\perp) = \langle \mathcal{P} e^{-ig_s \int_{-\infty}^{+\infty} dx^- A^+(x^-, x_\perp)} \rangle_A, \quad (5)$$

where $A^+ = A_c^+ t^c$ with t^c being the generators in the fundamental representation. Similarly, multiple scattering between incoming gluon (or eikonal line) and classical color field of the nucleus also can be resummed to all orders,

$$2\pi\delta(k^-)p^\mu[\tilde{U} - 1](k_\perp), \quad (6)$$

with

$$[\tilde{U} - 1](k_\perp) = \int d^2 x_\perp e^{-ik_\perp \cdot x_\perp} [\tilde{U}(x_\perp) - 1], \quad (7)$$

and

$$\tilde{U}(x_\perp) = \langle \mathcal{P} e^{-ig_s \int_{-\infty}^{+\infty} dx^- \tilde{A}^+(x^-, x_\perp)} \rangle_A, \quad (8)$$

where $(\tilde{A}^+)_{ab} = A_c^+(-if^{abc})$ with f^{abc} being the generators in the adjoint representation.

We use these as the building blocks to compute the amplitude for quark pair production in high energy pA collisions. It is straightforward to obtain the production amplitude for diagram(a) illustrated in the Fig.2,

$$\mathcal{M}^{(a)} = -ig_s \bar{u}(l_1) \gamma^\rho t^a \frac{l_2 - \not{k}_1 - m}{(l_2 - k_1)^2 - m^2 + i\epsilon} \not{p} [U^\dagger - 1](k_{1\perp}) v(l_2) \frac{\varepsilon_{\rho\sigma}(k_2)}{k_2^2 + i\epsilon} n^\sigma \frac{k_2 \cdot p}{p \cdot n} \phi_p(x_2, k_{2\perp}), \quad (9)$$

where the factor $2\pi\delta(k_1^-)$ is suppressed. $k_2 = l_1 + l_2 - k_1$ denotes the momentum of the gluon from the proton with l_1 and l_2 being the quark and anti-quark momentum, respectively. $\phi_p(x_2, k_{2\perp})$ represents the probability amplitude for finding a gluon carrying a certain momentum inside the proton, with $x_2 g(x_2, k_{2\perp}) = \phi_p \phi_p^*$. The other diagrams shown in Fig.2 give,

$$\mathcal{M}^{(b)} = -ig_s \bar{u}(l_1) \not{p} [U - 1](k_{1\perp}) \frac{l_1 - \not{k}_1 + m}{(l_1 - k_1)^2 - m^2 + i\epsilon} \gamma^\rho t^a v(l_2) \frac{\varepsilon_{\rho\sigma}(k_2)}{k_2^2 + i\epsilon} n^\sigma \frac{k_2 \cdot p}{p \cdot n} \phi_p(x_2, k_{2\perp}) \quad (10)$$

$$\begin{aligned} \mathcal{M}^{(c)} &= g_s \int \frac{d^4 k'_1}{(2\pi)^3} \delta(k'_1^-) \bar{u}(l_1) \not{p} [U - 1](k_{1\perp} - k'_{1\perp}) \frac{l_1 - \not{k}_1 + \not{k}'_1 + m}{(l_1 - k_1 + k'_1)^2 - m^2 + i\epsilon} \gamma^\rho t^a \\ &\quad \times \frac{l_2 - \not{k}'_1 - m}{(l_2 - k'_1)^2 - m^2 + i\epsilon} \not{p} [U^\dagger - 1](k'_{1\perp}) v(l_2) \frac{\varepsilon_{\rho\sigma}(k_2)}{k_2^2 + i\epsilon} n^\sigma \frac{k_2 \cdot p}{p \cdot n} \phi_p(x_2, k_{2\perp}) \end{aligned} \quad (11)$$

$$\mathcal{M}^{(d)} = -ig_s \bar{u}(l_1) \gamma^\rho t^b v(l_2) \frac{1}{k_1 \cdot n - i\epsilon} \frac{\varepsilon_{\rho\sigma}(k_2 + k_1)}{(k_2 + k_1)^2 + i\epsilon} n^\sigma \frac{(k_2 + k_1) \cdot p}{p \cdot n} [\tilde{U} - 1]_{ba}(k_{1\perp}) \phi_p(x_2, k_{2\perp}) \quad (12)$$

$$\mathcal{M}^{(e)} = -ig_s \bar{u}(l_1) \gamma^\rho t^b v(l_2) \frac{\varepsilon_{\rho\rho'}(k_2 + k_1)}{(k_2 + k_1)^2 + i\epsilon} \frac{\varepsilon_{\sigma\sigma'}(k_2)}{k_2^2 + i\epsilon} p^\mu \Lambda^{\mu\rho'\sigma'} n^\sigma \frac{k_2 \cdot p}{p \cdot n} [\tilde{U} - 1]_{ba}(k_{1\perp}) \phi_p(x_2, k_{2\perp}). \quad (13)$$

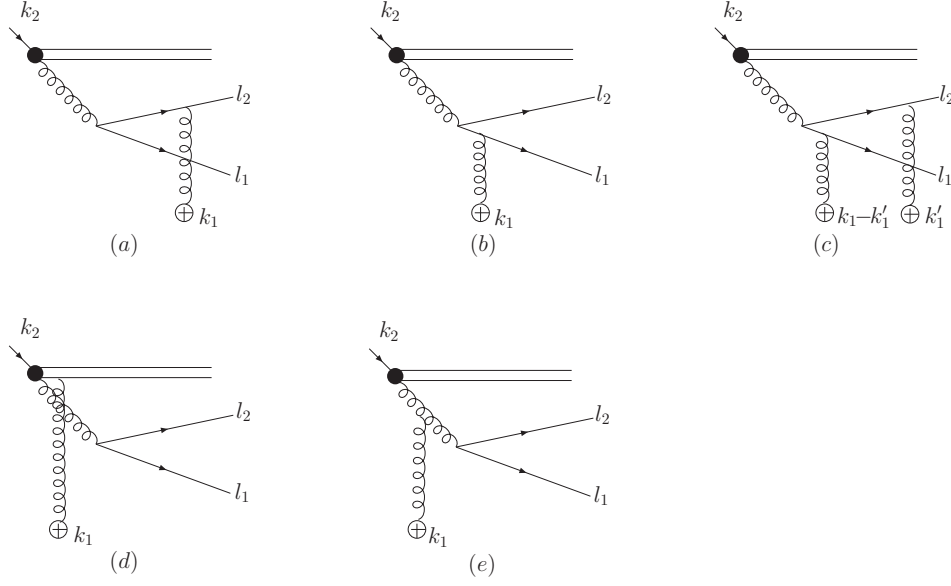


Figure 2: The diagrams contributing to quark pair production. The gluon line terminated by a \oplus denotes a classical field insertion. The contributions from all other diagrams disappear because the multiple poles are located in the same half plane.

Putting all these terms together, we obtain the following expression for the complete production amplitude,

$$\begin{aligned}
\mathcal{M} &= \mathcal{M}^{(a)} + \mathcal{M}^{(b)} + \mathcal{M}^{(c)} + \mathcal{M}^{(d)} + \mathcal{M}^{(e)} \\
&= g_s \int \frac{d^4 k'_1}{(2\pi)^3} \left\{ \delta(k'_1) \bar{u}(l_1) \not{p} \frac{l_1 - \not{k}_1 + \not{k}'_1 + m}{(l_1 - k_1 + k'_1)^2 - m^2 + i\epsilon} \gamma^\rho \frac{l_2 - \not{k}'_1 - m}{(l_2 - k'_1)^2 - m^2 + i\epsilon} \not{p} \right. \\
&\quad \times \left[U(k_{1\perp} - k'_{1\perp}) t^a U^\dagger(k'_{1\perp}) \right] v(l_2) \frac{\varepsilon_{\rho\sigma}(k_2)}{k_2^2 + i\epsilon} n^\sigma \frac{k_2 \cdot p}{p \cdot n} \phi_p(x_2, k_{2\perp}) \Big\} - i g_s \bar{u}(l_1) \gamma^\rho t^b v(l_2) \tilde{U}_{ba}(k_{1\perp}) \\
&\quad \times \left[\frac{\varepsilon_{\rho\rho'}(k_2 + k_1)}{(k_2 + k_1)^2 + i\epsilon} \frac{\varepsilon_{\sigma\sigma'}(k_2)}{k_2^2 + i\epsilon} p^\mu \Lambda^{\mu\rho'\sigma'} + \frac{1}{k_1 \cdot n - i\epsilon} \frac{\varepsilon_{\rho\sigma}(k_2 + k_1)}{(k_2 + k_1)^2 + i\epsilon} \right] n^\sigma \frac{k_2 \cdot p}{p \cdot n} \phi_p(x_2, k_{2\perp}) . \quad (14)
\end{aligned}$$

To arrive the above formula, we have made use of the Dirac equation of motion obeyed by the free spinors and the following identity for the Wilson lines in the different representations:

$$U(x_\perp) t^a U^\dagger(x_\perp) = t^b \tilde{U}^{ba}(x_\perp) . \quad (15)$$

After some algebraic, this production amplitude can be further rewritten in a more conventional form,

$$\begin{aligned}
\mathcal{M} &= i g_s \frac{k_2 \cdot p}{k_2^2} \phi_p(x_2, k_{2\perp}) \\
&\quad \times \bar{u}(l_1) \left\{ T_g(k_{1\perp}) t^b \tilde{U}_{ba}(k_{1\perp}) + \int \frac{d^2 k'_{1\perp}}{(2\pi)^2} \left[T_{q\bar{q}}(k_{1\perp}, k'_{1\perp}) U(k_{1\perp} - k'_{1\perp}) t^a U^\dagger(k'_{1\perp}) \right] \right\} v(l_2) \quad (16)
\end{aligned}$$

where,

$$T_{q\bar{q}}(k_{2\perp}, k_{1\perp}, k'_{1\perp}) = i \int \frac{dk'^- dk'^+}{2\pi} \delta(k'_1) \not{p} \frac{l_1 - \not{k}_1 + \not{k}'_1 + m}{(l_1 - k_1 + k'_1)^2 - m^2 + i\epsilon} \not{p} \frac{l_2 - \not{k}'_1 - m}{(l_2 - k'_1)^2 - m^2 + i\epsilon} \not{p} \quad (17)$$

$$T_g(k_{2\perp}, k_{1\perp}) = \frac{1}{(k_1 + k_2)^2} \left[\frac{k_{1\perp}^2 - (k_{1\perp} + k_{2\perp})^2}{k_2 \cdot p} \not{p} - \frac{k_{2\perp}^2}{k_1 \cdot n} \not{n} + 2 \not{k}_{2\perp} \right] - \frac{1}{k_2 \cdot p} \not{p} . \quad (18)$$

This result is in agreement with the production amplitude obtained in Ref. [16] up to a trivial prefactor. Note that $T_{q\bar{q}}(k_{2\perp} = 0, k_{1\perp}, k'_{1\perp}) + T_g(k_{2\perp} = 0, k_{1\perp}) = 0$.

Squaring the amplitude, we obtain the following expression for the pair production cross section,

$$\begin{aligned} \frac{d\sigma}{d\mathcal{P}.\mathcal{S}.} &= \frac{\alpha_s \pi}{N_c^2 - 1} \int \frac{2d^2 k_{1\perp}}{(2\pi)^3} d^2 k_{2\perp} \frac{d^2 k'_{1\perp} d^2 k''_{1\perp}}{(2\pi)^4} \frac{1}{(2\pi)^2} \delta^2(k_{1\perp} + k_{2\perp} - q_\perp) x_2 g(x_2, k_{2\perp}) \\ &\times \int d^2 x_\perp d^2 y_\perp d^2 x'_\perp d^2 y'_\perp e^{-ix_\perp \cdot (k_{1\perp} - k'_{1\perp})} e^{-iy_\perp \cdot k'_{1\perp}} e^{ix'_\perp \cdot (k_{1\perp} - k''_{1\perp})} e^{iy'_\perp \cdot k''_{1\perp}} \frac{1}{k_{2\perp}^2} \\ &\times \left\{ \text{Tr} \left[(\not{l}_1 + m) T_{q\bar{q}} (\not{l}_2 - m) \gamma^0 T_{q\bar{q}}^\dagger \gamma^0 \right] C(x_\perp, y_\perp, y'_\perp, x'_\perp) \right. \\ &\quad + \text{Tr} \left[(\not{l}_1 + m) T_{q\bar{q}} (\not{l}_2 - m) \gamma^0 T_g^\dagger \gamma^0 \right] C(x_\perp, y_\perp, y'_\perp, y'_\perp) \\ &\quad + \text{Tr} \left[(\not{l}_1 + m) T_g (\not{l}_2 - m) \gamma^0 T_{q\bar{q}}^\dagger \gamma^0 \right] C(x_\perp, x_\perp, y'_\perp, x'_\perp) \\ &\quad \left. + \text{Tr} \left[(\not{l}_1 + m) T_g (\not{l}_2 - m) \gamma^0 T_g^\dagger \gamma^0 \right] C(x_\perp, x_\perp, y'_\perp, y'_\perp) \right\}. \end{aligned} \quad (19)$$

where $g(x_2, k_{2\perp})$ denotes the un-integrated gluon distribution of a proton. In the phase space factor $d\mathcal{P}.\mathcal{S}. = d^2 l_{1\perp} d^2 l_{2\perp} dy_1 dy_2$, the quantities y_1, y_2 are the rapidities of the produced quark and anti-quark respectively. The quark pair imbalance is defined as $q_\perp = l_{1\perp} + l_{2\perp}$. The factor $2/(2\pi)^3$ associated with phase space integration is chosen such that for a single gluon target, $\int \frac{2d^2 k_{1\perp}}{(2\pi)^3} \frac{k_{1\perp}^2}{g^2 N_c} \langle \tilde{U}(k_{1\perp}) \tilde{U}^\dagger(k_{1\perp}) \rangle_{\text{gluon}} = x_1 \delta(1 - x_1)$ at lowest non-trivial order (see, for example, Ref. [42]). To obtain the above result, we have defined the normalization factor and the flux factor to be $k_{2\perp}^2 / (2k_2 \cdot p (N_c^2 - 1))$ and $1/(2k_2 \cdot p)$, respectively, rather than $k_{1\perp}^2 k_{2\perp}^2 / (4x_1 x_2 P_A \cdot P_B (N_c^2 - 1)^2)$, $1/(4x_1 x_2 P_A \cdot P_B)$ as used in Ref. [13], since the Lipatov approximation is only applied on the proton side. We have omitted the arguments of $T_{q\bar{q}}, T_g$. And $T'_{q\bar{q}}, T'_g$ denote the same quantities with $k'_{1\perp}$ replaced by $k''_{1\perp}$. The four point function $C(x_\perp, y_\perp, y'_\perp, x'_\perp)$ is defined as,

$$C(x_\perp, y_\perp, y'_\perp, x'_\perp) = \text{Tr}_c \left\langle U(x_\perp) t^a U^\dagger(y_\perp) U(y'_\perp) t^a U^\dagger(x'_\perp) \right\rangle_{x_1} \quad (20)$$

Here Tr_c is a trace over the color indices. The longitudinal momentum fraction of proton and nucleus carried by the incoming gluons are constrained by the kinematics,

$$x_1 = \frac{|l_{1\perp}| e^{-y_1} + |l_{2\perp}| e^{-y_2}}{\sqrt{s}}, \quad x_2 = \frac{|l_{1\perp}| e^{y_1} + |l_{2\perp}| e^{y_2}}{\sqrt{s}}, \quad (21)$$

where \sqrt{s} is the center of mass energy.

With this derived full CGC result, we proceed to the correlation limit where $|P_\perp| \equiv |l_{1\perp} - l_{2\perp}|/2 \gg |q_\perp|/2$. In this kinematical region, we may systemically neglect the terms suppressed by powers of $|k_{2\perp}|/|P_\perp|, |k_{1\perp}|/|P_\perp|$ and $Q_s/|P_\perp|$ in the four hard coefficients. We first perform a Taylor expansion of the hard coefficients in terms of $k_{2\perp}$. By dropping all terms suppressed by powers of $|k_{2\perp}|/|P_\perp|$, one ends up with,

$$\begin{aligned} \frac{d\sigma}{d\mathcal{P}.\mathcal{S}.} &\approx \frac{\alpha_s}{N_c^2 - 1} \int \frac{d^2 k_{1\perp}}{(2\pi)^4} d^2 k_{2\perp} \frac{d^2 k'_{1\perp} d^2 k''_{1\perp}}{(2\pi)^4} \delta^2(k_{1\perp} + k_{2\perp} - q_\perp) x_2 g(x_2, k_{2\perp}) \\ &\times \int d^2 x_\perp d^2 y_\perp d^2 x'_\perp d^2 y'_\perp e^{-ix_\perp \cdot (k_{1\perp} - k'_{1\perp})} e^{-iy_\perp \cdot k'_{1\perp}} e^{ix'_\perp \cdot (k_{1\perp} - k''_{1\perp})} e^{iy'_\perp \cdot k''_{1\perp}} \\ &\times \left\{ \text{Tr} \left[(\not{l}_1 + m) \bar{T}_{q\bar{q}} (\not{l}_2 - m) \gamma^0 \bar{T}_{q\bar{q}}^\dagger \gamma^0 \right]_{k_{2\perp}=0} C(x_\perp, y_\perp, y'_\perp, x'_\perp) \right. \\ &\quad \left. + \text{Tr} \left[(\not{l}_1 + m) \bar{T}_{q\bar{q}} (\not{l}_2 - m) \gamma^0 \bar{T}_g^\dagger \gamma^0 \right]_{k_{2\perp}=0} C(x_\perp, y_\perp, y'_\perp, y'_\perp) \right. \\ &\quad \left. + \text{Tr} \left[(\not{l}_1 + m) \bar{T}_g (\not{l}_2 - m) \gamma^0 \bar{T}_{q\bar{q}}^\dagger \gamma^0 \right]_{k_{2\perp}=0} C(x_\perp, x_\perp, y'_\perp, x'_\perp) \right. \\ &\quad \left. + \text{Tr} \left[(\not{l}_1 + m) \bar{T}_g (\not{l}_2 - m) \gamma^0 \bar{T}_g^\dagger \gamma^0 \right]_{k_{2\perp}=0} C(x_\perp, x_\perp, y'_\perp, y'_\perp) \right\}. \end{aligned}$$

$$\begin{aligned}
& +\text{Tr} \left[(\not{l}_1 + m) \bar{T}_g(\not{l}_2 - m) \gamma^0 \bar{T}_{q\bar{q}}^{\dagger'} \gamma^0 \right]_{k_{2\perp}=0} C(x_\perp, x_\perp, y'_\perp, x'_\perp) \\
& +\text{Tr} \left[(\not{l}_1 + m) \bar{T}_g(\not{l}_2 - m) \gamma^0 \bar{T}_g^{\dagger'} \gamma^0 \right]_{k_{2\perp}=0} C(x_\perp, x_\perp, y'_\perp, y'_\perp) \Big\} , \tag{22}
\end{aligned}$$

and with $\bar{T}_{q\bar{q}}, \bar{T}_g$ given by,

$$\bar{T}_{q\bar{q}}(k_{1\perp}, k'_{1\perp}) = i \int \frac{dk'^- dk'^+}{2\pi} \delta(k_1'^-) \not{p} \frac{\not{l}_1 - \not{k}_1 + \not{k}'_1 + m}{(\not{l}_1 - \not{k}_1 + \not{k}'_1)^2 - m^2 + i\epsilon} \frac{\hat{k}_{2\perp}}{(k_2 \cdot p)} \frac{\not{l}_2 - \not{k}'_1 - m}{(\not{l}_2 - \not{k}'_1)^2 - m^2 + i\epsilon} \not{p} \tag{23}$$

$$\bar{T}_g(k_{1\perp}) = \frac{1}{(k_1 + x_2 P_B)^2} \left[\frac{-2k_{1\perp} \cdot \hat{k}_{2\perp}}{k_2 \cdot p} \not{p} + 2\hat{k}_{2\perp} \right] , \tag{24}$$

where $\hat{k}_{2\perp} = k_{2\perp}/|k_{2\perp}|$ is a unit vector.

Now let's move on to discuss the power expansion on the nucleus side. The fact that the integration over $k'_{1\perp}, k''_{1\perp}$ are dominated by the kinematical region $k'_{1\perp} \sim k''_{1\perp} \sim Q_s$ — because the typical small x gluon transverse momentum is characterized by the saturation momentum — allows us to employ the power expansion in the correlation limit $Q_s \sim (k_{1\perp} + k_{2\perp})/2 \ll P_\perp$. To facilitate the power expansion, we replace $\bar{T}_{q\bar{q}}(k_{1\perp}, k'_{1\perp})$, $\bar{T}_g(k_{1\perp})$ with the following two expressions with the help of Ward identities (gauge invariance violation terms in the amplitude are proportional to the gluon off-shellness $\sim k_{1\perp}^2$, and thus can be neglected in the correlation limit.),

$$\begin{aligned}
& \bar{T}_{q\bar{q}}(k_{1\perp}, k'_{1\perp}) \Rightarrow \bar{T}_{q\bar{q}}(k_{1\perp}, k'_{1\perp}) \\
& -i \int \frac{dk'^- dk'^+}{2\pi} \delta(k_1'^-) \frac{\not{k}_1 - \not{k}'_1}{(x_1 - x'_1) P_A^+} \frac{\not{l}_1 - \not{k}_1 + \not{k}'_1 + m}{(\not{l}_1 - \not{k}_1 + \not{k}'_1)^2 - m^2 + i\epsilon} \frac{\hat{k}_{2\perp}}{(k_2 \cdot p)} \frac{\not{l}_2 - \not{k}'_1 - m}{(\not{l}_2 - \not{k}'_1)^2 - m^2 + i\epsilon} \frac{\not{k}'_1}{x'_1 P_A^+} \\
& \Rightarrow - \left[\frac{\gamma_i}{x_1 P_A^+} \frac{\not{l}_1 - \not{k}_1 + m}{(\not{l}_1 - \not{k}_1)^2 - m^2 + i\epsilon} \frac{\hat{k}_{2\perp}}{(k_2 \cdot p)} \right]_{k_{1\perp}=0} (k_{1\perp}^i - k_{1\perp}^i) \\
& - \left[\frac{\hat{k}_{2\perp}}{(k_2 \cdot p)} \frac{\not{l}_2 - \not{k}_1 - m}{(\not{l}_2 - \not{k}_1)^2 - m^2 + i\epsilon} \frac{\gamma_i}{x_1 P_A^+} \right]_{k_{1\perp}=0} k_{1\perp}^i + O\left(\frac{k_{1\perp}^2}{P_\perp^2}\right) \approx \tilde{T}_{q\bar{q},i}^A(k_{1\perp}^i - k_{1\perp}^i) + \tilde{T}_{q\bar{q},i}^B k_{1\perp}^i \tag{25}
\end{aligned}$$

$$\begin{aligned}
& \bar{T}_g(k_{1\perp}) \Rightarrow \bar{T}_g(k_{1\perp}) - \frac{1}{(k_1 + x_2 P_B)^2} \left(2 + \frac{k_{1\perp}^2}{x_1 x_2 P_A^+ P_B^-} \right) \hat{k}_{2\perp} \\
& \approx \left[\frac{1}{(k_1 + x_2 P_B)^2} \frac{-2\hat{k}_{2\perp,i}}{k_2 \cdot p} \not{p} \right]_{k_{1\perp}=0} k_{1\perp}^i = \tilde{T}_{g,i} k_{1\perp}^i , \tag{26}
\end{aligned}$$

with i denoting the transverse index. By making the above replacement, the differential cross section can be rewritten in the form,

$$\begin{aligned}
\frac{d\sigma}{d\mathcal{P}.S.} & \approx \frac{\alpha_s}{(N_c^2 - 1)} \int \frac{d^2 k_{1\perp} d^2 k_{2\perp}}{(2\pi)^4} \delta^2(k_{1\perp} + k_{2\perp} - q_\perp) x_2 g(x_2, k_{2\perp}) \int d^2 x_\perp d^2 x'_\perp e^{-ik_{1\perp} \cdot (x_\perp - x'_\perp)} \\
& \times \left\{ \text{Tr} \left[(\not{l}_1 + m) \tilde{T}_{q\bar{q},i}^A(\not{l}_2 - m) \gamma^0 \tilde{T}_{q\bar{q},j}^{A\dagger'} \gamma^0 \right]_{k_{2\perp}, k_{1\perp}=0} \left[\frac{\partial^2 C(x_\perp, y_\perp, y'_\perp, x'_\perp)}{\partial x_\perp^i \partial x_\perp'^j} \right]_{x_\perp=y_\perp, x'_\perp=y'_\perp} \right. \\
& + \text{Tr} \left[(\not{l}_1 + m) \tilde{T}_{q\bar{q},i}^A(\not{l}_2 - m) \gamma^0 \tilde{T}_{q\bar{q},j}^{B\dagger'} \gamma^0 \right]_{k_{2\perp}, k_{1\perp}=0} \left[\frac{\partial^2 C(x_\perp, y_\perp, y'_\perp, x'_\perp)}{\partial x_\perp^i \partial y_\perp'^j} \right]_{x_\perp=y_\perp, x'_\perp=y'_\perp} \\
& \left. + \text{Tr} \left[(\not{l}_1 + m) \tilde{T}_{q\bar{q},i}^B(\not{l}_2 - m) \gamma^0 \tilde{T}_{q\bar{q},j}^{A\dagger'} \gamma^0 \right]_{k_{2\perp}, k_{1\perp}=0} \left[\frac{\partial^2 C(x_\perp, y_\perp, y'_\perp, x'_\perp)}{\partial y_\perp^i \partial x_\perp'^j} \right]_{x_\perp=y_\perp, x'_\perp=y'_\perp} \right\}
\end{aligned}$$

$$\begin{aligned}
& +\text{Tr} \left[(\not{l}_1 + m) \tilde{T}_{q\bar{q},i}^B (\not{l}_2 - m) \gamma^0 \tilde{T}_{q\bar{q},j}^{B\dagger} \gamma^0 \right]_{k_{2\perp}, k_{1\perp}=0} \left[\frac{\partial^2 C(x_\perp, y_\perp, y'_\perp, x'_\perp)}{\partial y_\perp^i \partial y_\perp'^j} \right]_{x_\perp=y_\perp, x'_\perp=y'_\perp} \\
& +\text{Tr} \left[(\not{l}_1 + m) \tilde{T}_{q\bar{q},i}^A (\not{l}_2 - m) \gamma^0 \tilde{T}_{g,j}^{A\dagger} \gamma^0 \right]_{k_{2\perp}, k_{1\perp}=0} \left[\frac{\partial^2 C(x_\perp, y_\perp, x'_\perp, x'_\perp)}{\partial x_\perp^i \partial x_\perp'^j} \right]_{x_\perp=y_\perp} \\
& +\text{Tr} \left[(\not{l}_1 + m) \tilde{T}_{q\bar{q},i}^B (\not{l}_2 - m) \gamma^0 \tilde{T}_{g,j}^{B\dagger} \gamma^0 \right]_{k_{2\perp}, k_{1\perp}=0} \left[\frac{\partial^2 C(x_\perp, y_\perp, x'_\perp, x'_\perp)}{\partial y_\perp^i \partial x_\perp'^j} \right]_{x_\perp=y_\perp} \\
& +\text{Tr} \left[(\not{l}_1 + m) \tilde{T}_{g,i} (\not{l}_2 - m) \gamma^0 \tilde{T}_{q\bar{q},j}^{A\dagger} \gamma^0 \right]_{k_{2\perp}, k_{1\perp}=0} \left[\frac{\partial^2 C(x_\perp, x_\perp, y'_\perp, x'_\perp)}{\partial x_\perp^i \partial x_\perp'^j} \right]_{x'_\perp=y'_\perp} \\
& +\text{Tr} \left[(\not{l}_1 + m) \tilde{T}_{g,i} (\not{l}_2 - m) \gamma^0 \tilde{T}_{q\bar{q},j}^{B\dagger} \gamma^0 \right]_{k_{2\perp}, k_{1\perp}=0} \left[\frac{\partial^2 C(x_\perp, x_\perp, y'_\perp, x'_\perp)}{\partial x_\perp^i \partial y_\perp'^j} \right]_{x'_\perp=y'_\perp} \\
& +\text{Tr} \left[(\not{l}_1 + m) \tilde{T}_{g,i} (\not{l}_2 - m) \gamma^0 \tilde{T}_{g,j}^{A\dagger} \gamma^0 \right]_{k_{2\perp}, k_{1\perp}=0} \left[\frac{\partial^2 C(x_\perp, x_\perp, x'_\perp, x'_\perp)}{\partial x_\perp^i \partial x_\perp'^j} \right]_{x'_\perp=y'_\perp} \Bigg\} , \tag{27}
\end{aligned}$$

where the transverse momenta $k'_{1\perp}$ and $k''_{1\perp}$ have been integrated out. As a result, the four point functions collapse into the two point functions. The calculation of the Dirac traces in the above formula is rather easy, while the evaluation of the soft part in the McLerran-Venugopalan(MV) model is a bit more involved. In general, the tensor structure of the soft part can be decomposed in the following way,

$$\int \left[\frac{\partial^2 C(x_\perp, y_\perp, y'_\perp, x'_\perp)}{\partial x_{\perp,i} \partial x'_{\perp,j}} \right]_{x_\perp=y_\perp, x'_\perp=y'_\perp} = \frac{\delta_\perp^{ij}}{2} F_1(x_\perp, k_{1\perp}) + \left(\hat{k}_{1\perp}^i \hat{k}_{1\perp}^j - \frac{1}{2} \delta_\perp^{ij} \right) H_1(x_\perp, k_{1\perp}) . \tag{28}$$

where \int denotes $\int d^2 x_\perp d^2 x'_\perp e^{-ik_{1\perp} \cdot (x_\perp - x'_\perp)}$. $\hat{k}_{1\perp}^i$ is a unit vector $\hat{k}_{1\perp}^i \equiv k_{1\perp}^i / |k_{1\perp}|$, and $\delta_\perp^{ij} = -g^{ij} + (p^i n^j + p^j n^i) / p \cdot n$. The four point function $C(x_\perp, y_\perp, y'_\perp, x'_\perp)$ has been evaluated in the MV model in Ref. [16]. With the derived four point function, the coefficients F_i and H_i can be computed in a tedious but straightforward way. One finds,

$$F_1 = \int \left[\frac{\partial^2 C(x_\perp, y_\perp, y'_\perp, x'_\perp)}{\partial x_\perp^i \partial x_\perp'^j} \right]_{x_\perp=y_\perp, x'_\perp=y'_\perp} \delta_\perp^{ij} = \int \left[\frac{\partial^2 C(x_\perp, y_\perp, y'_\perp, x'_\perp)}{\partial y_\perp^i \partial y_\perp'^j} \right]_{x_\perp=y_\perp, x'_\perp=y'_\perp} \delta_\perp^{ij} \tag{29}$$

$$F_2 = \int \left[\frac{\partial^2 C(x_\perp, y_\perp, y'_\perp, x'_\perp)}{\partial x_\perp^i \partial y_\perp'^j} \right]_{x_\perp=y_\perp, x'_\perp=y'_\perp} \delta_\perp^{ij} = \int \left[\frac{\partial^2 C(x_\perp, y_\perp, y'_\perp, x'_\perp)}{\partial y_\perp^i \partial y_\perp'^j} \right]_{x_\perp=y_\perp, x'_\perp=y'_\perp} \delta_\perp^{ij} \tag{30}$$

$$\begin{aligned}
F_3 &= \int \left[\frac{\partial^2 C(x_\perp, x_\perp, y'_\perp, x'_\perp)}{\partial x_\perp^i \partial x_\perp'^j} \right]_{x'_\perp=y'_\perp} \delta_\perp^{ij} = \int \left[\frac{\partial^2 C(x_\perp, x_\perp, y'_\perp, x'_\perp)}{\partial y_\perp^i \partial x_\perp'^j} \right]_{x'_\perp=y'_\perp} \delta_\perp^{ij} \\
&= \int \left[\frac{\partial^2 C(x_\perp, y_\perp, x'_\perp, x'_\perp)}{\partial y_\perp^i \partial x_\perp'^j} \right]_{x_\perp=y_\perp} \delta_\perp^{ij} = \int \left[\frac{\partial^2 C(x_\perp, y_\perp, x'_\perp, x'_\perp)}{\partial y_\perp^i \partial x_\perp'^j} \right]_{x_\perp=y_\perp} \delta_\perp^{ij} \\
&= \frac{1}{2} \int \left[\frac{\partial^2 C(x_\perp, x_\perp, x'_\perp, x'_\perp)}{\partial x_\perp^i \partial x_\perp'^j} \right] \delta_\perp^{ij} , \tag{31}
\end{aligned}$$

and,

$$H_1 = \int \left[\frac{\partial^2 C(x_\perp, y_\perp, y'_\perp, x'_\perp)}{\partial x_{\perp,i} \partial x'_{\perp,j}} \right]_{x_\perp=y_\perp, x'_\perp=y'_\perp} \left(2\hat{k}_{1\perp}^i \hat{k}_{1\perp}^j - \delta_\perp^{ij} \right)$$

$$= \int \left[\frac{\partial^2 C(x_\perp, y_\perp, y'_\perp, x'_\perp)}{\partial y_\perp^i \partial y_\perp'^j} \right]_{x_\perp=y_\perp, x'_\perp=y'_\perp} \left(2\hat{k}_{1\perp}^i \hat{k}_{1\perp}^j - \delta_\perp^{ij} \right) \quad (32)$$

$$\begin{aligned} H_2 &= \int \left[\frac{\partial^2 C(x_\perp, y_\perp, y'_\perp, x'_\perp)}{\partial x_\perp^i \partial y_\perp'^j} \right]_{x_\perp=y_\perp, x'_\perp=y'_\perp} \left(2\hat{k}_{1\perp}^i \hat{k}_{1\perp}^j - \delta_\perp^{ij} \right) \\ &= \int \left[\frac{\partial^2 C(x_\perp, y_\perp, y'_\perp, x'_\perp)}{\partial y_\perp^i \partial y_\perp'^j} \right]_{x_\perp=y_\perp, x'_\perp=y'_\perp} \left(2\hat{k}_{1\perp}^i \hat{k}_{1\perp}^j - \delta_\perp^{ij} \right) \end{aligned} \quad (33)$$

$$\begin{aligned} H_3 &= \int \left[\frac{\partial^2 C(x_\perp, x_\perp, y'_\perp, x'_\perp)}{\partial x_\perp^i \partial x_\perp'^j} \right]_{x'_\perp=y'_\perp} \left(2\hat{k}_{1\perp}^i \hat{k}_{1\perp}^j - \delta_\perp^{ij} \right) \\ &= \int \left[\frac{\partial^2 C(x_\perp, x_\perp, y'_\perp, x'_\perp)}{\partial y_\perp^i \partial x_\perp'^j} \right]_{x'_\perp=y'_\perp} \left(2\hat{k}_{1\perp}^i \hat{k}_{1\perp}^j - \delta_\perp^{ij} \right) \\ &= \int \left[\frac{\partial^2 C(x_\perp, y_\perp, x'_\perp, x'_\perp)}{\partial y_\perp^i \partial x_\perp'^j} \right]_{x_\perp=y_\perp} \left(2\hat{k}_{1\perp}^i \hat{k}_{1\perp}^j - \delta_\perp^{ij} \right) \\ &= \int \left[\frac{\partial^2 C(x_\perp, y_\perp, x'_\perp, x'_\perp)}{\partial y_\perp^i \partial x_\perp'^j} \right]_{x_\perp=y_\perp} \left(2\hat{k}_{1\perp}^i \hat{k}_{1\perp}^j - \delta_\perp^{ij} \right) \\ &= \frac{1}{2} \int \left[\frac{\partial^2 C(x_\perp, x_\perp, x'_\perp, x'_\perp)}{\partial x_\perp^i \partial x_\perp'^j} \right] \left(2\hat{k}_{1\perp}^i \hat{k}_{1\perp}^j - \delta_\perp^{ij} \right), \end{aligned} \quad (34)$$

with,

$$F_1 = 2\pi^4 N_c \alpha_s x_1 \left[G_{DP}(x_1, k_{1\perp}) + \left(1 - \frac{4}{N_c^2} \right) G_{q\bar{q}}(x_1, k_{1\perp}) + \frac{2}{N_c^2} G_{WW}(x_1, k_{1\perp}) \right] \quad (35)$$

$$F_2 = 2\pi^4 N_c \alpha_s x_1 \left[G_{DP}(x_1, k_{1\perp}) - \left(1 - \frac{4}{N_c^2} \right) G_{q\bar{q}}(x_1, k_{1\perp}) - \frac{2}{N_c^2} G_{WW}(x_1, k_{1\perp}) \right] \quad (36)$$

$$F_3 = 2\pi^4 N_c \alpha_s x_1 [2G_{DP}(x_1, k_{1\perp})] \quad (37)$$

$$H_1 = 2\pi^4 N_c \alpha_s x_1 \left[h_{1,DP}^{\perp g}(x_1, k_{1\perp}) + \left(1 - \frac{4}{N_c^2} \right) h_{1,q\bar{q}}^{\perp g}(x_1, k_{1\perp}) + \frac{2}{N_c^2} h_{1,WW}^{\perp g}(x_1, k_{1\perp}) \right] \quad (38)$$

$$H_2 = 2\pi^4 N_c \alpha_s x_1 \left[h_{1,DP}^{\perp g}(x_1, k_{1\perp}) - \left(1 - \frac{4}{N_c^2} \right) h_{1,q\bar{q}}^{\perp g}(x_1, k_{1\perp}) - \frac{2}{N_c^2} h_{1,WW}^{\perp g}(x_1, k_{1\perp}) \right] \quad (39)$$

$$H_3 = 2\pi^4 N_c \alpha_s x_1 [2h_{1,DP}^{\perp g}(x_1, k_{1\perp})] . \quad (40)$$

To arrive at the results given above, we have neglected the logarithmic dependence of the saturation momentum on r_\perp^2 . $G_{DP}, G_{WW}, h_{1,DP}^{\perp g}$ and $h_{1,WW}^{\perp g}$ are the unpolarized gluon dipole distribution, the Weizsäcker-Williams (WW) type unpolarized gluon distribution, the dipole type linearly polarized gluon distribution, and the WW type linearly polarized gluon distribution, respectively. In the MV model, they read [28, 43, 44],

$$x_1 G_{DP}(x_1, k_{1\perp}) = x_1 h_{1,DP}^{\perp g}(x_1, k_{1\perp}) = \frac{C_F S_\perp}{2\pi^2 \alpha_s} k_{1\perp}^2 \int \frac{d^2 r_\perp}{(2\pi)^2} e^{-ik_{1\perp} \cdot r_\perp} e^{-\frac{r_\perp^2 Q_s^2}{4}} \quad (41)$$

$$x_1 G_{WW}(x_1, k_{1\perp}) = \frac{N_c^2 - 1}{N_c} \frac{S_\perp}{4\pi^4 \alpha_s} \int d^2 r_\perp e^{-ik_{1\perp} \cdot r_\perp} \frac{1}{r_\perp^2} \left(1 - e^{-\frac{r_\perp^2 Q_s^2}{4}} \right) \quad (42)$$

$$x_1 h_{1,WW}^{\perp g}(x_1, k_{1\perp}) = \frac{N_c^2 - 1}{8\pi^3} S_\perp \int dr_\perp \frac{J_2(|k_{1\perp}| |r_\perp|)}{\frac{1}{4\mu_A} |r_\perp| Q_s^2} \left(1 - e^{-\frac{r_\perp^2 Q_s^2}{4}} \right). \quad (43)$$

Here S_\perp is the transverse area of the target nucleus. $Q_s^2 = \alpha_s N_c \mu_A \ln [1/(r_\perp^2 \Lambda_{QCD}^2)]$ is the gluon saturation scale with μ_A being a common CGC parameter. J_2 is the second order Bessel function. Note that our convention for $h_{1,WW}^{\perp g}$ differs from that in Ref. [28] by a factor 1/2. The WW type gluon distributions have a clear physical interpretation as the number density of gluons inside a hadron/nucleus, while the dipole type distribution does not. On the other hand, the dipole type unpolarized gluon distribution in the adjoint representation enters the single gluon production cross section in pA collisions [45]. Besides these widely used gluon TMDs, two novel ones are given by,

$$x_1 G_{q\bar{q}}(x_1, k_{1\perp}) = \frac{C_F S_\perp}{2\pi^2 \alpha_s} \int \frac{d^2 r_\perp}{(2\pi)^2} e^{-ik_{1\perp} \cdot r_\perp} Q_s^2 e^{-\frac{r_\perp^2 Q_s^2}{4}}, \quad (44)$$

$$x_1 h_{1,q\bar{q}}^{\perp g}(x_1, k_{1\perp}) = \frac{N_c^2 - 1}{8\pi^3} S_\perp \int d|r_\perp| \mu_A |r_\perp| J_2(|k_{1\perp}| |r_\perp|) e^{-\frac{r_\perp^2 Q_s^2}{4}}. \quad (45)$$

Collecting all pieces together, the differential cross section for quark pair production can be written in the following general form,

$$\frac{d\sigma}{d\mathcal{P} \cdot \mathcal{S}} = \frac{\alpha_s^2 N_c}{\hat{s}^2 (N_c^2 - 1)} \left[\mathcal{A}(q_\perp^2) + \frac{m^2}{P_\perp^2} \mathcal{B}(q_\perp^2) \cos 2\phi + \mathcal{C}(q_\perp^2) \cos 4\phi \right] \quad (46)$$

where ϕ is the azimuthal angle between the transverse momenta q_\perp and P_\perp . The coefficients $\mathcal{A}(q_\perp^2)$, $\mathcal{B}(q_\perp^2)$ and $\mathcal{C}(q_\perp^2)$ contain convolutions of various gluon TMDs. Instead of presenting the full results for these coefficients, we neglect all higher powers in m^2/P_\perp^2 ,

$$\begin{aligned} \mathcal{A}(q_\perp^2) &= \int d^2 k_{1\perp} d^2 k_{2\perp} \delta^2(k_{1\perp} + k_{2\perp} - q_\perp) x_2 g(x_2, k_{2\perp}) \frac{(\hat{u}^2 + \hat{t}^2)}{4\hat{u}\hat{t}} \\ &\times \left\{ \frac{(\hat{t} - \hat{u})^2}{\hat{s}^2} x_1 G_{DP}(x_1, k_{1\perp}) + x_1 \left[\left(1 - \frac{4}{N_c^2}\right) G_{q\bar{q}}(x_1, k_{1\perp}) + \frac{2}{N_c^2} G_{WW}(x_1, k_{1\perp}) \right] \right\} \end{aligned} \quad (47)$$

$$\begin{aligned} \mathcal{B}(q_\perp^2) &= \int d^2 k_{1\perp} d^2 k_{2\perp} \delta^2(k_{1\perp} + k_{2\perp} - q_\perp) x_2 g(x_2, k_{2\perp}) \\ &\times \left\{ \left[2(\hat{k}_{1\perp} \cdot \hat{q}_\perp)^2 - 1 \right] \right. \\ &\times \left(\frac{(\hat{t} - \hat{u})^2}{\hat{s}^2} x_1 h_{1,DP}^{\perp g}(x_1, k_{1\perp}) + x_1 \left[\left(1 - \frac{4}{N_c^2}\right) h_{1,q\bar{q}}^{\perp g}(x_1, k_{1\perp}) + \frac{2}{N_c^2} h_{1,WW}^{\perp g}(x_1, k_{1\perp}) \right] \right) \\ &\left. + \left[2(\hat{k}_{2\perp} \cdot \hat{q}_\perp)^2 - 1 \right] \right. \\ &\times \left(\frac{(\hat{t} - \hat{u})^2}{\hat{s}^2} x_1 G_{DP}(x_1, k_{1\perp}) + x_1 \left[\left(1 - \frac{4}{N_c^2}\right) G_{q\bar{q}}(x_1, k_{1\perp}) + \frac{2}{N_c^2} G_{WW}(x_1, k_{1\perp}) \right] \right) \left. \right\} \end{aligned} \quad (48)$$

$$\begin{aligned} \mathcal{C}(q_\perp^2) &= \int d^2 k_{1\perp} d^2 k_{2\perp} \delta^2(k_{1\perp} + k_{2\perp} - q_\perp) x_2 g(x_2, k_{2\perp}) \\ &\times \left[\left(2(\hat{q} \cdot \hat{k}_{1\perp})(\hat{q} \cdot \hat{k}_{2\perp}) - \hat{k}_{1\perp} \cdot \hat{k}_{2\perp} \right)^2 - \frac{1}{2} \right] \\ &\times \left\{ \frac{(\hat{t} - \hat{u})^2}{\hat{s}^2} x_1 h_{1,DP}^{\perp g}(x_1, k_{1\perp}) + x_1 \left[\left(1 - \frac{4}{N_c^2}\right) h_{1,q\bar{q}}^{\perp g}(x_1, k_{1\perp}) + \frac{2}{N_c^2} h_{1,WW}^{\perp g}(x_1, k_{1\perp}) \right] \right\}, \end{aligned} \quad (49)$$

where $\hat{s} = (x_1 P_A + x_2 P_B)^2$, $\hat{t} = (x_2 P_B - l_1)^2$ and $\hat{u} = (x_1 P_A - l_1)^2$ are kinematical variables defined in the usual way. This is the main result of our paper, which opens the possibility to study saturation physics through measuring polarization observables as both unpolarized gluon TMDs and linearly polarized gluon TMDs are unambiguously determined in the MV model. In the end, we would like to mention that it is also feasible to take into account small x evolution effect [46, 47].

3 Dilute limit, forward limit, large N_c limit

In the correlation limit, the low gluon densities limit is reached in the kinematic region $Q_s^2 \ll k_{1\perp}^2 \ll P_\perp^2$. When $Q_s^2 \ll k_{1\perp}^2$, all six gluon distribution functions become identical, though they differ significantly at low $k_{1\perp}$,

$$\begin{aligned} x_1 G(x_1, k_{1\perp}) &\equiv x_1 h_{1,D\bar{P}}^{\perp g}(x_1, k_{1\perp}) = x_1 h_{1,WW}^{\perp g}(x_1, k_{1\perp}) = x_1 h_{1,q\bar{q}}^{\perp g}(x_1, k_{1\perp}) \\ &= x_1 G_{D\bar{P}}(x_1, k_{1\perp}) = x_1 G_{WW}(x_1, k_{1\perp}) = x_1 G_{q\bar{q}}(x_1, k_{1\perp}) \simeq S_\perp \frac{N_c^2 - 1}{4\pi^3} \frac{\mu_A}{k_{1\perp}^2}. \end{aligned} \quad (50)$$

Therefore, we have,

$$\begin{aligned} \mathcal{A}(q_\perp^2) &= \int d^2 k_{1\perp} d^2 k_{2\perp} \delta^2(k_{1\perp} + k_{2\perp} - q_\perp) x_2 g(x_2, k_{2\perp}) x_1 G(x_1, k_{1\perp}) \\ &\quad \times \left[\frac{N_c^2 - 1}{2N_c^2} \frac{\hat{u}^2 + \hat{t}^2}{\hat{u}\hat{t}} - \frac{\hat{t}^2 + \hat{u}^2}{\hat{s}^2} \right] \end{aligned} \quad (51)$$

$$\begin{aligned} \mathcal{B}(q_\perp^2) &= \int d^2 k_{1\perp} d^2 k_{2\perp} \delta^2(k_{1\perp} + k_{2\perp} - q_\perp) x_2 g(x_2, k_{2\perp}) x_1 G(x_1, k_{1\perp}) \\ &\quad \times 4 \left[\frac{N_c^2 - 1}{2N_c^2} - \frac{\hat{t}\hat{u}}{\hat{s}^2} \right] \left[2(\hat{k}_{1\perp} \cdot \hat{q}_\perp)^2 + 2(\hat{k}_{2\perp} \cdot \hat{q}_\perp)^2 - 2 \right] \end{aligned} \quad (52)$$

$$\begin{aligned} \mathcal{C}(q_\perp^2) &= \int d^2 k_{1\perp} d^2 k_{2\perp} \delta^2(k_{1\perp} + k_{2\perp} - q_\perp) x_2 g(x_2, k_{2\perp}) x_1 G(x_1, k_{1\perp}) \\ &\quad \times 4 \left[\frac{N_c^2 - 1}{2N_c^2} - \frac{\hat{t}\hat{u}}{\hat{s}^2} \right] \left[\left(2(\hat{q} \cdot \hat{k}_{1\perp})(\hat{q} \cdot \hat{k}_{2\perp}) - \hat{k}_{1\perp} \cdot \hat{k}_{2\perp} \right)^2 - \frac{1}{2} \right]. \end{aligned} \quad (53)$$

Here the known unpolarized Born cross section for $q\bar{q}$ production through gluon fusion has been recovered for the unpolarized term, as it should be. Agreement is also found between our results and the explicit expressions of the polarized cross section given in the papers [29,30], provided that these results are extended to the small x region and the same dilute limit is taken. Note that one automatically takes into account the linearly polarized gluons inside a proton in the Lipatov approximation. By observing these consistences, we conclude that in the dilute limit, the contribution to gluon TMDs from initial/final state interactions encoded in the gauge links can be neglected, and single gluon exchange dominates the processes.

Let us now discuss the expression in the forward limit. Since $k_{2\perp}$ is relatively small in the forward limit, we may make the approximation $\delta^2(k_{1\perp} + k_{2\perp} - q_\perp) \approx \delta^2(k_{1\perp} - q_\perp)$ and integrate out $k_{1\perp}$ and $k_{2\perp}$. This leads to the following simplified result,

$$\begin{aligned} \mathcal{A}(q_\perp^2) &= x_2 g(x_2) \frac{(\hat{u}^2 + \hat{t}^2)}{4\hat{u}\hat{t}} \\ &\quad \times \left\{ \frac{(\hat{t} - \hat{u})^2}{\hat{s}^2} x_1 G_{D\bar{P}}(x_1, q_\perp) + x_1 \left[\left(1 - \frac{4}{N_c^2} \right) G_{q\bar{q}}(x_1, q_\perp) + \frac{2}{N_c^2} G_{WW}(x_1, q_\perp) \right] \right\} \end{aligned} \quad (54)$$

$$\begin{aligned} \mathcal{B}(q_\perp^2) &= x_2 g(x_2) \\ &\quad \times \left\{ \frac{(\hat{t} - \hat{u})^2}{\hat{s}^2} x_1 h_{1,D\bar{P}}^{\perp g}(x_1, q_\perp) + x_1 \left[\left(1 - \frac{4}{N_c^2} \right) h_{1,q\bar{q}}^{\perp g}(x_1, q_\perp) + \frac{2}{N_c^2} h_{1,WW}^{\perp g}(x_1, q_\perp) \right] \right\} \end{aligned} \quad (55)$$

$$\mathcal{C}(q_\perp^2) = 0, \quad (56)$$

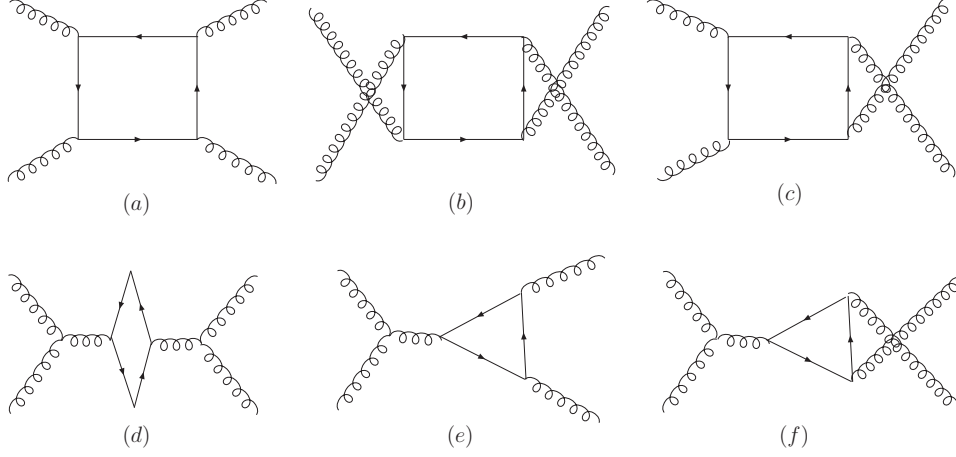


Figure 3: The diagrams contributing to quark pair production in TMD factorization approach. The gauge link structure of gluon TMD distributions associated with each diagram are different. The mirror diagrams are not shown.

where $g(x_2)$ is the integrated gluon distribution function for the proton. One finds that the $\cos 4\phi$ modulation drops out in the forward limit. In order to compare with the existing result for quark pair production in pA collisions in the forward limit, we further take the large N_c limit,

$$\mathcal{A}(q_\perp^2) = x_2 g(x_2) \frac{(\hat{u}^2 + \hat{t}^2)}{4\hat{u}\hat{t}} \left\{ \frac{(\hat{t} - \hat{u})^2}{\hat{s}^2} x_1 G_{DP}(x_1, q_\perp) + x_1 G_{q\bar{q}}(x_1, q_\perp) \right\} \quad (57)$$

$$\mathcal{B}(q_\perp^2) = x_2 g(x_2) \left\{ \frac{(\hat{t} - \hat{u})^2}{\hat{s}^2} x_1 h_{1,DP}^{\perp g}(x_1, q_\perp) + x_1 h_{1,q\bar{q}}^{\perp g}(x_1, q_\perp) \right\} \quad (58)$$

$$\mathcal{C}(q_\perp^2) = 0, \quad (59)$$

where the unpolarized cross section is in agreement with that obtained in Ref. [8] if one uses the relations $x_1 G_{DP}(x_1, q_\perp) = \mathcal{F}_{gg}^{(1)} - \mathcal{F}_{gg}^{(2)}$ and $x_1 G_{q\bar{q}}(x_1, q_\perp) = \mathcal{F}_{gg}^{(1)} + \mathcal{F}_{gg}^{(2)}$ valid in the large N_c limit. At this point, we would like to emphasize that the large N_c limit is not necessarily a good approximation. In particular, N_c suppressed terms are the dominant contribution in the dense medium since the various gluon TMDs scale as: $x_1 G_{DP}(x_1, k_{1\perp}) = x_1 h_{1,DP}^{\perp g}(x_1, k_{1\perp}) \sim k_{1\perp}^2/Q_s^2$, $x_1 G_{q\bar{q}}(x_1, k_{1\perp}) \sim 1$, $x_1 G_{WW}(x_1, k_{1\perp}) \sim \ln(Q_s^2/k_{1\perp}^2)$ and $x_1 h_{1,WW}^{\perp g}(x_1, k_{1\perp}) \sim x_1 h_{1,q\bar{q}}^{\perp g}(x_1, k_{1\perp}) \sim \mu_A/Q_s^2$ at low $k_{1\perp}$.

4 Quark pair production in TMD factorization

For quark pair production in hadronic collisions, generalized TMD factorization is not valid any longer as shown by presenting a direct counter-example in Ref. [6]. However, in pA collisions, if one only takes into account the interaction between the active partons and background gluon field inside a large nucleus while neglecting the longitudinal gluons attached to the proton side, the type of graph (for example, please see Fig.11 in the paper [6]) which can produce a violation of generalized TMD-factorization disappears. In this section, we use this approximation. Admittedly we cannot quantify the systematic errors introduced by it. After neglecting the extra gluon attachment on the proton side, the multiple gluon re-scattering between the hard part and the nucleus can be resummed to all orders in the form of a process dependent gauge link. Due to the different color structures, the gluon

TMDs associated with different Feynman diagrams correspond to different gauge link structures. For example, the gluon TMD correlation function associated with graph Fig.3(a) takes the form [48],

$$\begin{aligned} \Phi_{g,(a)}^{ij} &= 2 \int \frac{d\xi^- d\xi_\perp}{(2\pi)^3 P_A^+} e^{ix_1 P_A^+ - ik_{1\perp} \cdot \xi_\perp} \\ &\times \langle P | \text{Tr}_c \left\{ F^i(\xi) \left[\frac{N_c^2}{N_c^2 - 1} \frac{\text{Tr}[U[\square]^\dagger]}{N_c} U^{[-]\dagger} - \frac{1}{N_c^2 - 1} U^{[+]\dagger} \right] F^j(0) U^{[+]} \right\} | P \rangle, \end{aligned} \quad (60)$$

where i, j denote the gluon polarization index. The gauge links $U^{[+]}$, $U^{[-]}$ are defined as,

$$U^{[+]} = \mathcal{P} e^{-ig_s \int_0^\infty d\xi^- A^+(\xi^-, 0_\perp)} \mathcal{P} e^{-ig_s \int_\infty^{\xi^-} d\xi^- A^+(\xi^-, \xi_\perp)}, \quad (61)$$

$$U^{[-]} = \mathcal{P} e^{-ig_s \int_0^{-\infty} d\xi^- A^+(\xi^-, 0_\perp)} \mathcal{P} e^{-ig_s \int_{-\infty}^{\xi^-} d\xi^- A^+(\xi^-, \xi_\perp)}. \quad (62)$$

And $U[\square] = U^{[+]} U^{[-]\dagger} = U^{[-]\dagger} U^{[+]}$ emerges as a Wilson loop. At small x , this gluon TMD can be expressed as the derivative of a multiple-point function and subsequently be computed in the MV model. In order to derive this relation, we made use of the Fierz identities,

$$\begin{aligned} C(x_\perp, y_\perp, y'_\perp, x'_\perp) &= \text{Tr}_c \langle U(x_\perp) t^a U^\dagger(y_\perp) U(y'_\perp) t^a U^\dagger(x'_\perp) \rangle \\ &= \frac{1}{2} \text{Tr}_c \langle U^\dagger(x'_\perp) U(x_\perp) \rangle \text{Tr}_c \langle U^\dagger(y_\perp) U(y'_\perp) \rangle - \frac{1}{2N_c} \text{Tr}_c \langle U(x_\perp) U^\dagger(y_\perp) U(y'_\perp) U^\dagger(x'_\perp) \rangle, \end{aligned} \quad (63)$$

and the formula,

$$\partial^i U(x_\perp) = -ig_s \int_{-\infty}^\infty dx^- U[-\infty, x^-, x_\perp] \partial^i A^+(x^-, x_\perp) U[x^-, \infty, x_\perp]. \quad (64)$$

With the help of the above two identities, one finds,

$$\Phi_{(a)}^{ij} = \frac{2N_c}{N_c^2 - 1} \frac{2}{\alpha_s} \int \frac{d^2 x_\perp d^2 x'_\perp}{(2\pi)^4} e^{-ik_{1\perp}(x_\perp - x'_\perp)} \left[\frac{\partial^2}{\partial x_{\perp,i} \partial x'_{\perp,j}} C(x_\perp, y_\perp, y'_\perp, x'_\perp) \right]_{x_\perp=y_\perp, x'_\perp=y'_\perp} \quad (65)$$

The normalization on the right hand side of the equation is fixed according to the arguments made in Ref. [8]. Following a similar procedure, for the gluon distribution correlation functions associated with other diagrams shown in Fig.3, we obtain,

$$\Phi_{(b)}^{ij} = \frac{2N_c}{N_c^2 - 1} \frac{2}{\alpha_s} \int \frac{d^2 x_\perp d^2 x'_\perp}{(2\pi)^4} e^{-ik_{1\perp}(x_\perp - x'_\perp)} \left[\frac{\partial^2}{\partial y_{\perp,i} \partial y'_{\perp,j}} C(x_\perp, y_\perp, y'_\perp, x'_\perp) \right]_{x_\perp=y_\perp, x'_\perp=y'_\perp} \quad (66)$$

$$\Phi_{(c)}^{ij} = 2N_c \frac{2}{\alpha_s} \int \frac{d^2 x_\perp d^2 x'_\perp}{(2\pi)^4} e^{-ik_{1\perp}(x_\perp - x'_\perp)} \left[\frac{\partial^2}{\partial x_{\perp,i} \partial y'_{\perp,j}} C(x_\perp, y_\perp, y'_\perp, x'_\perp) \right]_{x_\perp=y_\perp, x'_\perp=y'_\perp} \quad (67)$$

$$\Phi_{(d)}^{ij} = \frac{1}{N_c} \frac{2}{\alpha_s} \int \frac{d^2 x_\perp d^2 x'_\perp}{(2\pi)^4} e^{-ik_{1\perp}(x_\perp - x'_\perp)} \left[\frac{\partial^2}{\partial x_{\perp,i} \partial x'_{\perp,j}} C(x_\perp, x_\perp, x'_\perp, x'_\perp) \right] \quad (68)$$

$$\Phi_{(e)}^{ij} = \frac{2}{N_c} \frac{2}{\alpha_s} \int \frac{d^2 x_\perp d^2 x'_\perp}{(2\pi)^4} e^{-ik_{1\perp}(x_\perp - x'_\perp)} \left[\frac{\partial^2}{\partial x_{\perp,i} \partial x'_{\perp,j}} C(x_\perp, x_\perp, y'_\perp, x'_\perp) \right]_{x'_\perp=y'_\perp} \quad (69)$$

$$\Phi_{(f)}^{ij} = \frac{2}{N_c} \frac{2}{\alpha_s} \int \frac{d^2 x_\perp d^2 x'_\perp}{(2\pi)^4} e^{-ik_{1\perp}(x_\perp - x'_\perp)} \left[\frac{\partial^2}{\partial x_{\perp,i} \partial y'_{\perp,j}} C(x_\perp, x_\perp, y'_\perp, x'_\perp) \right]_{x'_\perp=y'_\perp} \quad (70)$$

With these relations, all of the unpolarized and linearly polarized gluon TMDs can be calculated in the MV model. On the other hand, it is straightforward to compute the partonic hard cross section contributions from each diagram in the Fig.3. Combining the derived gluon TMDs and hard parts and summing the contributions from all diagrams, we obtain the final result in the TMD factorization framework. In order to compare the obtained TMD factorization result with that calculated in the CGC formalism, we have to take the same dilute limit on the proton side, which means that the unpolarized gluon distribution and the linearly polarized gluon distribution inside a proton become identical. After making this assumption, a perfect matching between the CGC formalism and TMD factorization is found in the correlation limit. Note that this conclusion is valid beyond the large N_c limit.

5 Summary

In this paper, we have studied quark pair production in high energy proton-nucleus collisions in the central rapidity region and in the correlation limit where the total transverse momentum of the quark pair (q_\perp) is much smaller than the transverse momenta of the individual quarks ($\approx P_\perp$). Our main focus lay on the polarized case. We first used a hybrid approach to reproduce the full CGC result for quark pair production beyond the correlation limit. Our hybrid approach allowed us to take into account finite gluon transverse momentum effect on the proton side in a certain approximation. Employing a power expansion in the correlation limit, the multiple-point functions appearing in the full CGC result collapse into two-point functions and are thus given by a combination of gluon TMDs. All finite N_c terms are kept in our calculation. The resulting cross section contains $\cos 2\phi$ and $\cos 4\phi$ dependent terms, where ϕ is azimuthal angle between the transverse momenta q_\perp and P_\perp . In addition to WW and dipole type linearly polarized gluon distributions, the novel linearly polarized gluon distribution $h_{1,q\bar{q}}^{\perp g}$ also accounts for $\cos 2\phi$ and $\cos 4\phi$ modulations. Such observables in principal can be measured at RHIC and LHC.

We further discussed our results in the dilute limit, the forward limit and the large N_c limit, and found consistency with existing results in the different limits. The physical implications of the observed consistences were also addressed. In the end, we showed that a calculation based on TMD factorization leads to the same result as obtained in the hybrid approach. The technique introduced in this paper can be extended to study di-jet production in the other channels for pA collisions (e.g. di-jets initiated by different partons and/or various polarization channels). For these the linearly polarized gluon TMDs with different gauge link structures may also manifest themselves through $\cos 2\phi$ or $\cos 4\phi$ azimuthal dependences of the cross sections. We would expect that exploring these polarization observables at small x could open a new path in spin physics as well as in saturation physics.

Acknowledgments: One of us (Jian Zhou) thanks Andreas Metz for suggesting this work to him and for helpful discussions. This work has been supported by BMBF (OR 06RY9191).

References

- [1] J. C. Collins and D. E. Soper, Nucl. Phys. B **193**, 381 (1981) [Erratum-ibid. B **213**, 545 (1983)] [Nucl. Phys. B **213**, 545 (1983)]; Nucl. Phys. B **194**, 445 (1982). J. C. Collins, D. E. Soper and G. F. Sterman, Nucl. Phys. B **250**, 199 (1985).
- [2] X. -d. Ji, J. -p. Ma and F. Yuan, Phys. Rev. D **71**, 034005 (2005) [hep-ph/0404183].

- [3] D. Boer, M. Diehl, R. Milner, R. Venugopalan, W. Vogelsang, D. Kaplan, H. Montgomery and S. Vigdor *et al.*, arXiv:1108.1713 [nucl-th].
- [4] M. Anselmino *et al.*, Eur. Phys. J. A **47**, 35 (2011) [arXiv:1101.4199 [hep-ex]].
- [5] J. Collins and J. -W. Qiu, Phys. Rev. D **75**, 114014 (2007) [arXiv:0705.2141 [hep-ph]].
- [6] T. C. Rogers and P. J. Mulders, Phys. Rev. D **81**, 094006 (2010) [arXiv:1001.2977 [hep-ph]].
- [7] F. Dominguez, B. W. Xiao and F. Yuan, Phys. Rev. Lett. **106**, 022301 (2011) [arXiv:1009.2141 [hep-ph]].
- [8] F. Dominguez, C. Marquet, B. W. Xiao and F. Yuan, Phys. Rev. D **83**, 105005 (2011) [arXiv:1101.0715 [hep-ph]].
- [9] E. Avsar, arXiv:1203.1916 [hep-ph].
- [10] P. Nason, S. Dawson and R. K. Ellis, Nucl. Phys. B **303**, 607 (1988); Nucl. Phys. B **327**, 49 (1989) [Erratum-ibid. B **335**, 260 (1990)].
- [11] S. Frixione, M. L. Mangano, P. Nason and G. Ridolfi, Adv. Ser. Direct. High Energy Phys. **15**, 609 (1998) [hep-ph/9702287].
- [12] S. Catani, M. Ciafaloni, F. Hautmann, Nucl. Phys. **B366**, 135-188 (1991).
- [13] J. C. Collins, R. K. Ellis, Nucl. Phys. **B360**, 3-30 (1991).
- [14] E. M. Levin, M. G. Ryskin, Y. .M. Shabelski and A. G. Shuvaev, Sov. J. Nucl. Phys. **53**, 657 (1991) [Yad. Fiz. **53**, 1059 (1991)].
- [15] F. Gelis and R. Venugopalan, Phys. Rev. D **69**, 014019 (2004) [hep-ph/0310090].
- [16] J. P. Blaizot, F. Gelis, R. Venugopalan, Nucl. Phys. **A743**, 57-91 (2004). [hep-ph/0402257].
- [17] A. Schafer and J. Zhou, Phys. Rev. D **85**, 114004 (2012) [arXiv:1203.1534 [hep-ph]].
- [18] L. D. McLerran and R. Venugopalan, Phys. Rev. D **49**, 2233 (1994) [arXiv:hep-ph/9309289]; Phys. Rev. D **49**, 3352 (1994) [arXiv:hep-ph/9311205].
- [19] A. H. Mueller, arXiv:hep-ph/0111244.
- [20] E. A. Kuraev, L. N. Lipatov, V. S. Fadin, Sov. Phys. JETP **45**, 199-204 (1977).
- [21] L. V. Gribov, E. M. Levin, M. G. Ryskin, Phys. Rept. **100**, 1-150 (1983).
- [22] P. J. Mulders and J. Rodrigues, Phys. Rev. D **63**, 094021 (2001) [arXiv:hep-ph/0009343].
- [23] M. Anselmino, M. Boglione, U. D'Alesio, E. Leader, S. Melis and F. Murgia, Phys. Rev. D **73**, 014020 (2006) [hep-ph/0509035].
- [24] S. Meissner, A. Metz and K. Goeke, Phys. Rev. D **76**, 034002 (2007) [arXiv:hep-ph/0703176].
- [25] D. Boer and P. J. Mulders, Phys. Rev. D **57**, 5780 (1998) [arXiv:hep-ph/9711485].
- [26] S. J. Brodsky, D. S. Hwang and I. Schmidt, Phys. Lett. B **530**, 99 (2002) [arXiv:hep-ph/0201296].
- [27] J. C. Collins, Phys. Lett. B **536**, 43 (2002) [arXiv:hep-ph/0204004].

- [28] A. Metz, J. Zhou, Phys. Rev. **D84**, 051503 (2011). [arXiv:1105.1991 [hep-ph]].
- [29] D. Boer, P. J. Mulders and C. Pisano, Phys. Rev. D **80**, 094017 (2009) [arXiv:0909.4652 [hep-ph]].
- [30] D. Boer, S. J. Brodsky, P. J. Mulders and C. Pisano, Phys. Rev. Lett. **106**, 132001 (2011) [arXiv:1011.4225 [hep-ph]].
- [31] J. -W. Qiu, M. Schlegel and W. Vogelsang, Phys. Rev. Lett. **107**, 062001 (2011) [arXiv:1103.3861 [hep-ph]].
- [32] D. Boer, W. J. den Dunnen, C. Pisano, M. Schlegel and W. Vogelsang, Phys. Rev. Lett. **108**, 032002 (2012) [arXiv:1109.1444 [hep-ph]].
- [33] P. Sun, B. -W. Xiao, F. Yuan, Phys. Rev. **D84**, 094005 (2011). [arXiv:1109.1354 [hep-ph]].
- [34] T. Liou, arXiv:1206.6123 [hep-ph].
- [35] D. Boer and C. Pisano, arXiv:1208.3642 [hep-ph].
- [36] S. Catani, M. Grazzini, Nucl. Phys. **B845**, 297-323 (2011). [arXiv:1011.3918 [hep-ph]].
- [37] S. Mantry, F. Petriello, Phys. Rev. **D81**, 093007 (2010). [arXiv:0911.4135 [hep-ph]]; and references therein.
- [38] P. M. Nadolsky, C. Balazs, E. L. Berger, C. -P. Yuan, Phys. Rev. **D76**, 013008 (2007). [hep-ph/0702003 [HEP-PH]].
- [39] M. Garcia-Echevarria, A. Idilbi and I. Scimemi, arXiv:1111.4996 [hep-ph]. M. G. Echevarria, A. Idilbi, A. Schäfer and I. Scimemi, arXiv:1208.1281 [hep-ph].
- [40] I. Balitsky, Nucl. Phys. **B463**, 99-160 (1996). [hep-ph/9509348].
- [41] L. D. McLerran, R. Venugopalan, Phys. Rev. **D59**, 094002 (1999). [hep-ph/9809427].
- [42] E. Iancu, A. Leonidov and L. McLerran, arXiv:hep-ph/0202270.
- [43] Y. V. Kovchegov, Phys. Rev. D **54**, 5463 (1996) [arXiv:hep-ph/9605446].
- [44] J. Jalilian-Marian, A. Kovner, L. D. McLerran and H. Weigert, Phys. Rev. D **55**, 5414 (1997) [arXiv:hep-ph/9606337].
- [45] Y. V. Kovchegov, A. H. Mueller, Nucl. Phys. **B529**, 451-479 (1998). [hep-ph/9802440]. B. Z. Kopeliovich, A. V. Tarasov, A. Schäfer, Phys. Rev. **C59**, 1609-1619 (1999). [hep-ph/9808378]. A. Dumitru, L. D. McLerran, Nucl. Phys. **A700**, 492-508 (2002). [hep-ph/0105268]. J. P. Blaizot, F. Gelis, R. Venugopalan, Nucl. Phys. **A743**, 13-56 (2004). [hep-ph/0402256].
- [46] J. Jalilian-Marian, A. Kovner, A. Leonidov, H. Weigert, Phys. Rev. **D59**, 014014 (1999). [hep-ph/9706377]. J. Jalilian-Marian, A. Kovner, A. Leonidov, H. Weigert, Nucl. Phys. **B504**, 415-431 (1997). [hep-ph/9701284]. E. Iancu, A. Leonidov, L. D. McLerran, Nucl. Phys. **A692**, 583-645 (2001). [hep-ph/0011241]. E. Ferreira, E. Iancu, A. Leonidov, L. McLerran, Nucl. Phys. **A703**, 489-538 (2002). [hep-ph/0109115].

- [47] A. Dumitru, J. Jalilian-Marian, Phys. Rev. **D81**, 094015 (2010). [arXiv:1001.4820 [hep-ph]]; Phys. Rev. **D82**, 074023 (2010) [arXiv:1008.0480 [hep-ph]]. F. Dominguez, A. H. Mueller, S. Munier, B. -W. Xiao, Phys. Lett. **B705**, 106-111 (2011). [arXiv:1108.1752 [hep-ph]]. F. Dominguez, J. -W. Qiu, B. -W. Xiao and F. Yuan, Phys. Rev. D **85**, 045003 (2012) [arXiv:1109.6293 [hep-ph]]. A. Dumitru, J. Jalilian-Marian, T. Lappi, B. Schenke and R. Venugopalan, Phys. Lett. B **706**, 219 (2011) [arXiv:1108.4764 [hep-ph]]. E. Iancu and D. N. Triantafyllopoulos, JHEP **1111**, 105 (2011) [arXiv:1109.0302 [hep-ph]]. JHEP **1204**, 025 (2012) [arXiv:1112.1104 [hep-ph]].
- [48] C. J. Bomhof, P. J. Mulders and F. Pijlman, Phys. Lett. B **596**, 277 (2004) [hep-ph/0406099]; Eur. Phys. J. C **47**, 147 (2006) [hep-ph/0601171].